PCCP

RSC Publishing

PERSPECTIVE

View Article Online
View Journal | View Issue

Single-molecule assays for investigating protein misfolding and aggregation

Cite this: *Phys. Chem. Chem. Phys.*, 2013, **15**, 7934

Armin Hoffmann,[a] Krishna Neupane[a] and Michael T. Woodside*[ab]

Received 18th December 2012,
Accepted 11th April 2013

DOI: 10.1039/c3cp44564j

www.rsc.org/pccp

Protein misfolding and aggregation are relevant to many fields. Recently, their investigation has experienced a revival as a central topic in the research of numerous human diseases, including Parkinson's and Alzheimer's. Much has been learned from ensemble biochemical approaches, but the inherently heterogeneous nature of the underlying processes has obscured many important details. Single-molecule techniques offer unique capabilities to study heterogeneous systems, while providing high temporal and structural resolution to characterize them. In this Perspective, we give an overview of the single-molecule assays that have been applied to protein misfolding and aggregation, which are mainly based on fluorescence and force spectroscopy. We describe some of the technical challenges involved in studying aggregation at the single-molecule level and discuss what has been learned about aggregation mechanisms from the different approaches.

Introduction

How proteins misfold and assemble into non-native aggregates is a question of wide importance, affecting fields ranging from biophysics and cell biology to biotechnology and medicine.[1] At a fundamental level, aggregation is believed to be a general feature of protein sequences, and therefore competes with native folding.[2] This leads to an important role in the evolution of protein sequences: protein sequences and folding mechanisms are not only optimized for specific structures and functions, but also to avoid misfolding and consequent dysfunction.[3] Misfolding and aggregation play important roles at the cellular level, too: their prevention is an aspect of many essential processes, such as protein expression,[4] stress response (in particular by the action of chaperones),[5] protein degradation,[6] and aggregate processing.[7] In the context of biotechnology, aggregation can cause significant yield losses during recombinant protein production, as an undesired by-product when refolding protein isolated from inclusion bodies,[8] and it can also cause problems during the storage[9] and application of proteins,

[a] *Department of Physics, University of Alberta, Edmonton, AB, Canada*
[b] *National Institute for Nanotechnology, 11421 Saskatchewan Dr., Edmonton, AB T6G 2M9, Canada. E-mail: Michael.Woodside@nrc-cnrc.gc.ca*

Armin Hoffmann

Armin Hoffmann graduated in Biotechnology at the Mannheim University of Applied Sciences in Germany. He received his PhD in Biochemistry from the University of Zurich, Switzerland under the supervision of Prof. Ben Schuler, and is now a postdoctoral fellow with Prof. Woodside. He is interested in protein folding and misfolding, techniques such as single-molecule fluorescence and force spectroscopy, as well as in related data analysis methods.

Krishna Neupane

Krishna Neupane graduated from Tribhuvan University, Nepal. He received his PhD in Physics from Kent State University, USA, studying light scattering in liquid crystals with Prof. Samuel Sprunt. As a postdoctoral fellow with Prof Michael Woodside, he has studied nucleic acid as well as protein misfolding and aggregation at the single-molecule level with optical tweezers.

for instance biopharmaceuticals.[10] On the other hand, aggregation can sometimes be useful, as when controlled native aggregation is used to tune pharmacokinetics in long-acting insulin variants.[11] Finally, misfolding and aggregation play a central role in a wide range of diseases, from Alzheimer's and Parkinson's to systemic amyloidosis, transmissible spongiform encephalopathies, and forms of diabetes.[12] A common characteristic of misfolding diseases is the presence of fibrillar deposits called amyloids consisting of specific proteins in a misfolded, cross-β arrangement.[13,14] Originally, amyloids were believed to be pathogenic, but increasing evidence suggests that in many misfolding diseases toxicity arises mainly from smaller oligomeric aggregates.[15–17] Interestingly, amyloids have also been identified as being a native and functional conformation of some proteins.[18] Despite the growing interest in native aggregation, in this Perspective we concentrate on non-native aggregation, since the latter remains the primary focus of much protein aggregation research, especially in the single-molecule regime.

Aggregation characteristics

Aggregation† is a process of almost bewildering complexity. It may start from monomers that are natively-structured, partially-denatured, or misfolded; different numbers of monomers may associate to form oligomers of various sizes, with the monomer conformations remodeled within oligomers in different ways. Oligomers may in turn grow into larger aggregates, whether amorphous or highly-structured as in the case of amyloid fibrils (Fig. 1A).[19] Given this complexity, describing aggregation at the molecular level is a technically daunting task. Three of the principal goals for investigating protein misfolding and aggregation are: (1) to identify and characterize the different structural species formed by misfolded and aggregated proteins; (2) to elucidate the network of pathways connecting these different species, determine the transition rates between them, and identify the important intermediates; and (3) to understand the effect of protein modifications, co-factors, and various solution or environmental conditions on the first two points.

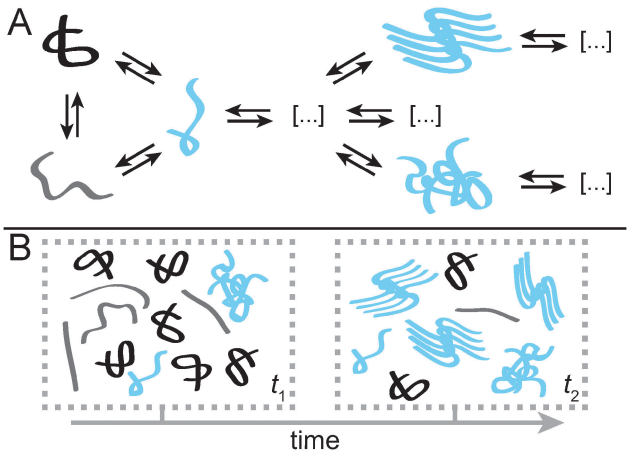

Fig. 1 Simplified schematic of protein aggregation. (A) As a competing reaction to the native folding process (gray: unfolded. black: folded), a misfolded conformation (blue) may form, which subsequently may oligomerize into amorphous (lower right) or highly ordered (upper right) structures. Many other species may also occur (ellipses). (B) Over the course of the aggregation, many different states are simultaneously populated, here illustrated by mostly monomeric conformations at early times and mostly oligomeric conformations at later times.

The first step is to identify and characterize the species which are present at different stages of the aggregation. Specific structures may play different important roles, for example acting as key intermediates during aggregation, causing cytotoxicity or infection, or acting as protective agents by clearing the toxic species. The structural features of these species will influence properties such as their protease resistance and solubility. Other key characteristics include the rate at which the species dissociate from or associate to larger structures and their ability to bind to other proteins, cellular factors, or membranes; the latter may influence their toxicity, *e.g.* by membrane pore formation[20] or the disturbance of crucial cellular functions.[21] The "mobility" of a species, *i.e.* its localization within a cell[22] and ability to transmit between cells,[23] organs,[24] or whole organisms,[25] is also a crucial property, since it may impact disease propagation and is thus of central interest in the prion-like behavior of many misfolding diseases.[26–28]

Mapping the kinetic pathways connecting all the possible states is another important goal, since identifying the rate-limiting steps is crucial for understanding the aggregation mechanism.[29,30] Given the complexity of the aggregation landscape, a distribution of species is expected to arise from different stages of aggregation along a given pathway as well as different, competing pathways, producing a "molecular menagerie" (Fig. 1B).[31] Hence the properties of an aggregating protein will be determined by an ensemble of states whose composition changes in time. Importantly, the species in this ensemble which give rise to the most prominent structural characteristics might not be the ones which are responsible for other critical features like toxicity. An interesting question

† For clarity, we define "aggregation" as the association of multiple copies of a protein with at least partially non-native structures into a larger complex, whereas "misfolding" denotes the adoption by a single protein molecule of a structure that is not on the native folding pathway.

Michael T. Woodside

Michael Woodside is a Senior Research Officer at the National Institute for Nanotechnology and an Assistant Professor of Physics at the University of Alberta. He received a PhD in Physics from UC Berkeley. His research focuses on structure formation in the single-molecule regime. Recent work includes measurements of folding energy landscapes using force spectroscopy, studies of mRNA folding as it relates to gene regulation, and high-resolution assays of protein misfolding and aggregation.

regarding the pathways concerns the nature of the monomeric, aggregation-prone species,[32] which might be different when initializing aggregation as compared to propagating existing aggregates.

Finally, there are a great many factors that can influence the aggregation behavior. For example, changes in the protein itself, such as point mutations (especially in the context of diseases[33,34]) or post-translational modifications (*e.g.* glycosylation[35] or phosphorylation[36]), can alter the aggregation kinetics, the structures formed, and their properties. The presence of co-factors or changes in solution conditions (such as temperature, pH, ionic strength, denaturant, specific metal ions, osmophobic effects,[37] molecular chaperones,[5] and macromolecular crowding[38]) can also affect the aggregation.[39] These effects can be sufficiently dramatic that they ultimately lead to completely different aggregation behavior, *e.g.* formation of amorphous aggregates as opposed to ordered amyloids.

Benefits of single-molecule approaches

Many of the standard techniques used to study protein folding have also been used to investigate aggregation.[40–43] However, these approaches involve averaging over the ensemble of states present in the sample at a given time. Such averaging can present challenges for interpretation, because key states may be hidden within the ensemble if they are only populated rarely or briefly. Single-molecule methods‡ provide a promising new approach to overcome the technical challenges posed by misfolding and aggregation. By monitoring molecules or particles one at a time, the effects of ensemble averaging can be avoided. Subpopulations in a heterogeneous ensemble can be identified and characterized individually, and very rare events can be observed directly. Single molecules or particles can often be tracked over time, allowing the network of intermediate states to be mapped. Proteins can also be studied at low concentrations, allowing the initial stages of aggregation to be studied since the formation of larger aggregates is disfavored. Such techniques have been applied to obtain important insights into native protein folding,[44,45] yielding information including the folding pathways, energetic and kinetic properties of states, structural characteristics of intermediates, and properties of the folding landscape.

Here we focus on the use of single-molecule fluorescence spectroscopy and single-molecule force spectroscopy to study aggregation. We briefly outline the general principles of each method, describe the most common strategies to study protein misfolding and aggregation in more detail, and review the results obtained to date from their application. In particular, we describe assays based on fluorescence correlation spectroscopy, fluorescence intensity, Förster resonance energy transfer, and fluorescence bleaching, as well as forced-based assays for studying monomer misfolding, oligomerization in tandem-repeat proteins, and inter- or intra-molecular interactions within aggregates ranging from dimers to amyloid fibrils. We also briefly introduce nanopore analysis, another single-molecule technique that has recently been applied to protein misfolding.

Single-molecule fluorescence spectroscopy

Single-molecule fluorescence spectroscopy is based on measuring the time-dependent fluorescence from individual molecules, typically in the context of confocal or total internal reflection microscopy. The general technical requirements and methods for implementing fluorescence assays have been reviewed elsewhere.[46–48] We focus here on some of the requirements which are of special interest when studying protein aggregation. In most cases, fluorescent dyes with high quantum yields must be attached to the molecule of interest to achieve the required signal strength. The dye attachment not only increases the technical challenge for preparing samples, but may also alter the aggregation behavior of the protein. As a useful control, the behavior of labeled proteins may be compared with that of unlabeled proteins using ensemble methods. Another characteristic of single-molecule fluorescence measurements is that the labeled molecules must be present at very low concentration (typically 10^{-9}–10^{-11} M). Although a very dilute sample is advantageous for studying monomer misfolding, aggregation studies typically need much higher protein concentrations. These conflicting requirements can be resolved by adding a small amount of labeled protein to an excess of unlabeled protein, for example. To observe the small signals from single molecules, measurements are typically made in solutions with low background fluorescence, usually simple aqueous buffers, although the effects of more complex environments—including live cells—are increasingly being studied.[49]

Different approaches have been used to observe single molecules with fluorescence.[50] In some assays, the proteins of interest are attached to the surface of the microscope cover glass directly, *via* covalent linkages (Fig. 2A). Other approaches

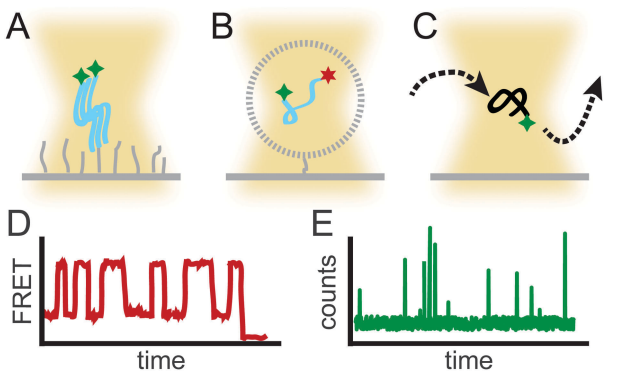

Fig. 2 Schematic representation of single-molecule fluorescence spectroscopy approaches. (A) The molecules can be tethered within the confocal excitation volume (yellow) directly to a cover glass (gray), (B) encapsulated in a tethered micro-cavity, or (C) allowed to diffuse freely in solution and then detected when passing through the confocal volume. (D) Immobilized molecules can be observed for longer times to reveal conformational changes, for example using FRET. (E) Freely-diffusing molecules are detected as short bursts of photons.

‡ Since aggregates consist of more than one molecule, some authors avoid speaking of "single-molecule" approaches, using terms like "single-oligomer" or "single-particle" instead. The technical requirements and implementation are however very similar whether studying small, single complexes or single molecules. Our use of "single-molecule" should be understood as referring to the techniques rather than the objects of study.

to immobilizing the proteins include enclosing them in microcavities (such as lipid vesicles) tethered to the cover glass (Fig. 2B) or placing them in porous gel matrices. In all these cases, single molecules are detected as spots with high fluorescence intensity, which can be monitored over extended times (typically until the fluorescent dye bleaches, see Fig. 2D). Alternatively, the molecules can be observed as they diffuse freely in solution (Fig. 2C), thereby avoiding the technical challenges of immobilization and especially the potential perturbation to the behavior of the protein or dyes that may result from it.[51] Here, the molecules are detected when they traverse the detection volume, resulting in a short burst of photons (Fig. 2E). The observation times are shorter than for immobilized molecules, but this effect can be compensated in part by confining the molecules using electrokinetic means[52] or capillaries,[53] or by applying special analytical methods, *e.g.* examining the recurrence behavior of the molecules.[54] Each approach can be combined with fluid-exchange techniques for changing the solution conditions,[55] from simple flow chambers to rapid micro-fluidic mixers for non-equilibrium measurements with dead times of milliseconds and lower.[56]

To distinguish between subpopulations at the monomer level or during the aggregation, several aspects of the fluorescence signal can be monitored, for instance the brightness and the lifetime of the dyes, spectral characteristics, time correlations,[57] polarization anisotropy,[58] quenching, and Förster resonance energy transfer (FRET).[59] These parameters can report on properties such as the number of dye molecules, their diffusion and rotational time constants, the distance between FRET or quencher pairs, and the relative motions between such pairs.[60] Often, a single fluorescence observable may reflect the effects of several different properties of the protein and/or dye, requiring that the mixture of contributions be disentangled carefully.

The main applications of single-molecule fluorescence to study aggregation have been: (i) characterization of the aggregation process, especially the time-dependent distributions of oligomers, and how it is altered by additional factors; (ii) ultra-sensitive detection of disease related aggregates; and (iii) identification and characterization of misfolded proteins, especially as precursors of aggregation. Many of these studies have focused on proteins associated with diseases, including α-synuclein[61] (Parkinson's disease), amyloid-β (Alzheimer's disease), and prion proteins[62] (spongiform encephalopathies). We discuss below examples of the main approaches and what they have revealed about protein aggregation.

Investigating aggregation by fluorescence correlation spectroscopy

One of the principal methods with single-molecule resolution that has been applied to study the aggregation process is fluorescence correlation spectroscopy (FCS). FCS makes use of the intensity fluctuations in the fluorescence signal from dye-labeled molecules as they diffuse through a small excitation volume (Fig. 2C and E).[63,64] In aggregation studies with FCS, typically a mixture of unlabeled and labeled proteins is used (on the order of 100 : 1 to 1000 : 1). The correlations in the fluorescence signal are analyzed to obtain information about the labeled particles such as their diffusion time and concentration (see Fig. 3A). Since diffusion times depend on both the size and shape of the particles, they can in principle be used to estimate the number of monomers per particle. Diffusion parameters may even be extracted for multiple species in a mixture, in cases where the diffusion times are sufficiently different. In cases where the subpopulation information is difficult to extract, the average signal can still be used as an indicator of the progress of the aggregation. A high sensitivity to the presence of small oligomers, as well as to their size and concentration, makes this technique especially suited to monitor early events in the aggregation process.

In one of the first FCS studies of aggregation, Post and colleagues analyzed the structural conversion and initial oligomerization of hamster prion protein.[65] After initializing aggregation, the authors found that the average diffusion time increased noticeably. They resolved three kinetic phases which

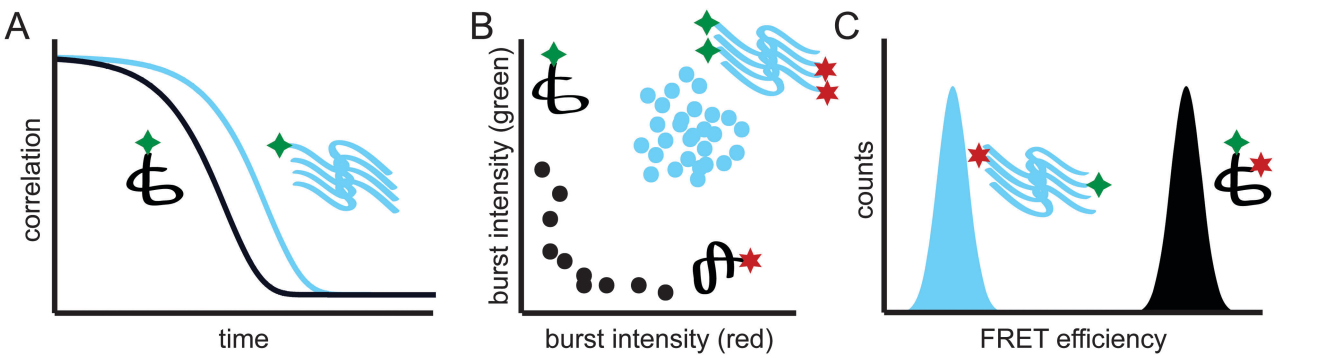

Fig. 3 Schematic representation of results from single-molecule fluorescence assays. Monomeric forms of the protein are shown in black, oligomeric forms in blue; dye labels are shown in green or red. (A) Auto-correlation functions from FCS. The slower diffusion time of oligomers (blue) shifts the decay of the correlation signal to longer times, compared to a monomer (black). (B) Scatter-plot from dual-probe intensity assay of a sample containing molecules labelled with one of two different dyes (green/four-pointed star or red/six-pointed star). Bursts from monomers (black) appear near the axes, since each monomer is labeled with only a single color, whereas bursts from oligomers (blue) have high intensity in both channels, since oligomers tend to include multiple copies of each dye. (C) Histogram from FRET measurements. Different intramolecular distances (or other factors, see text) arising from different conformations produce different levels of apparent FRET efficiency. In this case, a compact native monomer (black) produces high FRET efficiency, in contrast to the low efficiency from a more extended conformation within an aggregate (blue).

were interpreted, based on the values of the diffusion times, as a fast initial dimerization (occurring in the dead time of the kinetic measurement), subsequent formation of intermediate-sized oligomers, and finally slow formation of large, heterogeneous multimers.

Studying the aggregation of amyloid-β (aβ), Tjernberg *et al.* were able to resolve two main species simultaneously, relating them respectively to monomeric and oligomeric forms of the protein.[66] They found that the oligomeric fraction increased rapidly at first, then stabilized, and finally decreased in concert with a decreasing diffusion time for the largest species. They also tested the effects of small peptide ligands, which in some cases inhibited the oligomerization. The authors mentioned possible uncertainties in determining the fractions of the different species, since the number and brightness of the dyes within the aggregates were unknown. In a separate study of aβ, the Maiti group investigated the formation of different oligomer species.[67] Using maximum-entropy analysis of the correlation spectra,[68] they obtained the distributions of different species present during the aggregation, thereby also resolving two main populations. The same group also extended the application of FCS to the cellular environment, studying aβ aggregation on and close to cell membranes.[69] In contrast to very small oligomers in the extracellular space, larger oligomers could be identified at nM concentrations on the membranes.

The effects of specific proteins on the aggregation of α-synuclein were studied by Gerard *et al.* by monitoring average diffusion times.[70] Several α-synuclein-binding proteins were shown to accelerate aggregation, an effect which could be counteracted by including additional proteins that inhibited the binding. Nath and colleagues investigated the early steps of oligomer formation by α-synuclein, as well as subsequent oligomer dissociation, using a different analytical approach:[71] instead of taking the average diffusion time, they calculated the diffusion time for each 10 s segment within the data record and examined the distribution of these diffusion times as aggregation proceeded. They found a prevalence of fast diffusion times (indicating monomeric α-synuclein) shortly after inducing aggregation, shifting to slower diffusion after a couple of hours, indicating the presence of oligomeric states. After inducing oligomer dissociation by raising the pH, the dissociation rates could be quantified from the change in the distribution of diffusion times.

These studies show that FCS is a useful tool for probing the early stages of aggregation. However, care must be taken in analyzing the correlation functions. It is known that the average diffusion time found from FCS can be biased by experimental effects (*e.g.* due to distortions of the detection volume or optical saturation of the dyes).[72–74] Extracting the distribution of species present is also non-trivial, even in systems with only two populations, where the accuracy of the results depends on the relative concentrations of the two components and their fluorescence quantum yield.[74,75] Although quantitative analysis of the aggregating species may be difficult, FCS has nevertheless proven to be a valuable tool for detecting early intermediates, their temporal progression, and at least their qualitative properties. The incorporation of new technical developments promises continuing improvements in the accuracy of FCS results.[73] For example, the use of two confocal volumes separated by a known distance allows for the measurement of much more accurate diffusion times,[76] whereas extending FCS to include other probes like fluorescent state lifetimes can improve the subpopulation resolution.[77]

Investigating aggregation using fluorescence intensity

Rather than monitoring the fluorescence fluctuations, the fluorescence signal from individual molecules may be measured directly. In this case, the concentration of labeled molecules is lower than in classic FCS, typically in the 10–100 pM range, to ensure that only one molecule (or aggregate) is measured at a time. The molecules are detected either as a burst of photons (for freely-diffusing samples) or as a spot with high fluorescence intensity (for immobilized samples), and the fluorescence characteristics of each one can then be used to distinguish subpopulations. One primary characteristic used in this way is the fluorescence intensity, which depends (among other factors) on the number of fluorescently-labeled proteins per particle. The fraction of labeled proteins can be tuned simply by changing the ratio of labeled to unlabeled protein. Aggregates can thus in principle be identified and characterized by their high fluorescence intensity.

This assay was applied to detect the presence of aggregates as a marker of disease, where the high sensitivity is particularly useful. For example, Pitschke and colleagues identified aβ aggregates in the cerebrospinal fluid (CSF) of Alzheimer's patients using this approach.[78] CSF fluid samples were found to seed rapid aggregation of labeled aβ peptides added to the sample, as indicated by the fast appearance of bursts with high intensity; the rate of large bursts was about ten times lower in CSF from control patients or unseeded samples.

Bieschke and colleagues later introduced some refinements to improve the assay reliability (terming the method scanning for intensely fluorescent targets or SIFT).[79] First, instead of letting samples diffuse freely in solution, they were enclosed in a capillary and moved through the confocal volume. This approach makes the detection efficiency less dependent on particle size (since the time spent in the detection volume is dominated by the capillary movement, not the diffusion constants of the molecules) and increases the assay throughput. Second, they labeled antibodies instead of the target protein, allowing direct detection of aggregates in the CSF sample without having to seed a new round of aggregation, which could give false positives from self-aggregation of the labeled protein. The use of antibodies allows the bursts to be related to specific structural features, but prevents detection of conformations for which the antibody is not specific or where the target epitope is buried. Larger aggregates would still be expected to produce bursts with higher intensity, since they can bind more antibodies. The third improvement was that two fluorescent probes were used instead of just one, in this case two antibodies targeting different epitopes and labeled with different dyes. Both dyes could be excited and detected simultaneously,

increasing the sensitivity since aggregates should produce high-intensity bursts at both dye emission wavelengths simultaneously. The signals from the dual-probe assay are visualized in a scatter plot, displaying the intensity in the two detection channels for each burst. As illustrated in Fig. 3B, regions with low photon count rates in both detector channels represent unbound antibodies, regions with high burst rates in one channel and low burst rates in the other channel represent either non-specific binding to other particles or self-aggregation of the probes, and the region with high photon rates in both channels (*i.e.* large coincident bursts) represents specific binding.

This assay was first applied to detect prion protein aggregation. Analysis of brain samples from scrapie-infected hamsters confirmed very sensitive detection of prion protein aggregates; measurements of CSF from human patients with Creutzfeld–Jacob disease showed a significant signal in $\sim$20% of the cases, compared to 0% for the control group.[79] The assay was also applied to detect prion protein aggregates in both scrapie-infected hamster and cattle infected by bovine spongiform encephalopathy, again showing significantly more high-intensity coincident bursts in infected samples than non-infected ones.[80] A similar assay was also applied to detect aβ aggregates in CSF from Alzheimer's patients. In this case, the aggregates were immobilized on the microscope cover-glass *via* antibodies to improve detection efficiency and lower the signal background, by washing the sample before measurement.[81]

Beyond their use for detecting the presence of disease-related aggregates, burst-intensity assays have also been applied to study the mechanism of aggregation. Giese and colleagues probed α-synuclein aggregation using a mixture of protein that was either unlabeled or labeled with one of two dyes.[82] Based on two-channel scatter plots for detecting the characteristic signature of aggregation, they found that adding β-synuclein significantly inhibited aggregation, as indicated by fewer large coincident bursts. Experiments with mixtures of wild-type protein and a mutant associated with familial Parkinson's disease (each labeled with one of the dyes) found that they co-aggregated, with aggregation enhanced for mixtures at ratios of 5 : 1 or 1 : 5. To ensure a more uniform detection efficiency independent of particle size, the confocal measuring volume was scanned rapidly through the sample (analogous to the capillary scanning above[79]). The same method was later used to study the effects of various solvent conditions and additives on the aggregation of prion protein,[83] α-synuclein,[84–86] tau protein,[87] and NOTCH3.[88]

A similar dual-probe photon-burst method, termed two color coincidence detection (TCCD), was used by Orte and colleagues to characterize the aggregation of the SH3 domain of the PI3 kinase.[89] They found a very fast association of monomers concomitant with an increase in the fraction of oligomeric species. Moreover, the oligomers were found to have increasing stability against dissociation as aggregation proceeded. A key feature of the TCCD approach is that the sample contains only labeled protein, rather than a mixture of labeled and unlabeled proteins. The fluorescence intensity of any particle will then be proportional to the number of dye labels and can be used to infer the number of monomers per particle. However, this approach poses a number of technical challenges. Since all proteins are to be labeled, it is essential to ensure that the labeling does not affect the aggregation process. To achieve single-molecule conditions ($\sim 10^{-11}$ M), the sample needs to be diluted significantly after aggregating at high concentration ($\sim 10^{-5}$ M), requiring that dissociation processes be included in the interpretation. For example, the dissociation rates observed for SH3 domain oligomers were on the order of 1 h^{-1}, whereas the measurements after dilution took 1 h.[89] In addition to the number of dye labels, the fluorescence intensity also depends on factors such as quenching, rotational restrictions, or energy transfer, which can all blur the relationship between intensity and number of monomers. These other factors may be identified by measuring fluorescence anisotropy or lifetime, as done for SH3-domain fibrils.

TCCD was also used to investigate the effects of the chaperone clusterin on aβ aggregation.[90] A characteristic distribution was observed wherein the abundance of an oligomer decayed exponentially with oligomer size under all conditions. Adding clusterin at the start of aggregation inhibited the formation of any oligomers, whereas adding it at later times merely halted the formation of additional oligomers. Moreover, complexes between oligomers and clusterin were found to be very stable. As an extension to the previous application of TCCD, the authors used an oscillating stage to scan the confocal measurement volume over the sample, thereby decreasing the influence of differential diffusion rates on the detection efficiency of different oligomers.

These studies clearly show the powerful possibilities for detecting and studying protein aggregation provided by single-molecule fluorescence spectroscopy. They also reveal the technical challenges that must be overcome to quantify either the number of species present or the number of monomers per particle. The detection efficiency is different for different species, *e.g.* owing to changes in the diffusion times or brightness, which will bias the measured distributions. The dye brightness can change substantially in different environments, *e.g.* in a monomer *versus* an aggregate. This relationship is further blurred by the fact that different diffusion paths through the detection volume lead to different photon rates for the same molecule due to variations in the excitation intensity. These and other effects must be accounted for by appropriate control experiments. Such shortcomings have been partially addressed, for instance by moving the stage or the confocal volume fast to reduce the effect of the diffusion time on the detection efficiency. The incorporation of additional fluorescence parameters will further improve the accuracy of the description of oligomer distributions during the early steps of aggregation.

Characterizing misfolded and aggregated states

While information on the intensity of photon bursts can reveal the size of the particles in the sample, other methods can be used to characterize the states involved in more detail, especially techniques like FRET for probing molecular distances (Fig. 3C).

Single-molecule FRET has revealed many new and important insights into protein folding,[59] but its application to protein misfolding and aggregation has been rare. The principles of single-molecule FRET have been reviewed elsewhere.[48] Briefly, FRET involves non-radiative energy transfer from a donor to an acceptor fluorescent dye, with an efficiency that depends strongly on the inter-dye distance (with a low distance resulting in a high efficiency and *vice versa*). The efficiency also depends on other properties such as the donor fluorescence quantum yield, the relative orientation of the dyes, their spectra, and the refractive index. These parameters are less likely to be affected when an isolated molecule changes conformation, but they may change when the dye is incorporated into an aggregate: for example, fluorescence quenching is more likely to occur and dyes are more likely to be constrained rotationally, possibly to different degrees in different aggregates. Such variations introduce challenges for relating FRET efficiency to the inter-dye distance in the context of aggregation. As a result, whereas FRET usually yields quantitative information at the monomer level, results for aggregation may be more qualitative. Some of the ambiguities for interpreting FRET efficiency may be resolved by recording additional parameters alongside with FRET efficiency (*e.g.* fluorescence lifetime and anisotropy), yielding additional information about the molecules and dyes.

Two general modes of FRET measurements can be distinguished. In the first, the two dyes are attached to the same molecule. Here, the intra-molecular FRET can report on conformational changes due to misfolding or upon incorporation into an oligomer. In the second, the two dyes are attached to different molecules which are then mixed together, similar to the fluorescence intensity assays described in the previous section. Measurements of inter-molecular FRET between molecules in a complex can report on the conformations of oligomeric species themselves.

Several studies have used FRET to investigate the conformations of monomeric α-synuclein that may be relevant for aggregation. One study revealed different, site-specific effects of various aggregation-promoting conditions. Whereas low pH promoted chain collapse in the C-terminus of the protein (as indicated by high efficiency between a FRET pair in this region), binding of charged molecules showed only minor effects, suggesting an influence later in the aggregation process.[91] Another study found different structural features for a disease-related mutant of α-synuclein in the presence of SDS; the wild-type had an elongated structure at mM SDS concentrations, but the mutant was more flexible and less structured.[92]

Single-molecule FRET probes were also used to observe and characterize transient misfolding in the folding of tandem immunoglobulin domains from the I band of titin.[93] Titin is naturally a tandem-repeat protein, in which the repeated domains are connected end-to-end. Measurements of the refolding of tandem dimers showed that when the two domains had high sequence similarity, a small population (a few percent) adopted misfolded conformations with domain-swapped β-strands. In contrast, when the dimer contained domains with lower sequence similarity, no misfolding was observed.

An overview of the characteristics of aggregates in FRET experiments is described in a study by Hillger *et al.*[94] In refolding measurements of rhodanese, two structural species were identified: folded molecules with a high intra-molecular FRET efficiency, and aggregated molecules with intermediate intra-molecular FRET efficiency. The latter showed a significant increase in the average value and variance of photon burst durations, as expected for larger molecules diffusing more slowly through the confocal volume. The aggregates also had a higher anisotropy value, indicating a lower rotational mobility of the dye, and a reduced acceptor lifetime, possibly caused by quenching in the aggregate. A combination of FRET with TCCD was also applied to α-synuclein aggregation.[95] Going beyond monitoring the change in the size of oligomers (from TCCD analysis), the inter-molecular FRET efficiency between monomers within the oligomers was used as an additional criterion to differentiate oligomeric subspecies.

These studies show that FRET can provide detailed structural information of subpopulations in the case of monomeric proteins. In the context of aggregates, such structural information is more difficult to extract. Nevertheless, even qualitative information can be very useful for differentiating subpopulations. In future work it may be possible to relate FRET efficiency to detailed structural models with the help of other fluorescent parameters.[60]

Oligomer sizes from bleaching steps

A different approach that has been used to quantify the number of monomers in single oligomers is to monitor photo-bleaching. The bleaching of single fluorescent dyes is expected to result in discrete, quantized decreases in the fluorescence emission. The number of bleaching steps can be directly related to the number of dyes in the observed particle. This method thus sidesteps many of the technical challenges described above, since it is less dependent on the absolute magnitude of the fluorescence brightness. The principal requirements for photo-bleaching analysis are a high degree of labeling per monomer and an immobilization of the sample. The bleaching approach was applied to study early events in aggregation of aβ, characterizing the distributions of oligomer sizes under various conditions.[96,97]

Single-molecule force spectroscopy

Single-molecule force spectroscopy uses a force probe to apply tension as a denaturant to the molecule of interest. Structural changes in response to the force, such as unfolding, are monitored by measuring changes in the end-to-end extension of the molecule. The force is applied between two specific points on the protein defined by the attachments to the force probe. Commonly-used probes include the atomic force microscope (AFM), optical tweezers, and magnetic tweezers, which have all been reviewed extensively elsewhere.[98,99] AFM is best suited when high forces are required (especially 100 pN or higher), whereas optical and magnetic tweezers are best when low forces are needed (especially 50 pN or below). AFM and

optical tweezers measurements are typically made over timescales from minutes to hours (limited, for instance, by their sensitivity to instrumental drift). Magnetic tweezers may be used for longer measurements (hours to days), but to our knowledge they have not yet been applied to study protein misfolding or aggregation. An important difference between the techniques is the geometry. With an AFM, the proteins are typically attached directly between the tip of a cantilever and a functionalized surface,[100] whereas with optical tweezers, the proteins are usually connected *via* DNA handles to small beads, which in turn are held by lasers. Measuring the changes in the length of the molecule with sufficient resolution for structural characterization requires high-precision instrumentation, which can be achieved for both AFM and optical tweezers but requires careful attention to the experimental and instrumental design.[101]

Several different types of assays for studying aggregation can be distinguished based on the experimental geometry (Fig. 4). Monomer misfolding can be studied by connecting a single monomer to the force probe (Fig. 4A). Intermolecular interactions in aggregates can be studied by attaching a protein to the probe and bringing it into contact with another molecule (Fig. 4B), or by using the probe to pull on individual monomers incorporated into an aggregate (Fig. 4C). Monomers can also be linked into a single chain to form tandem repeats for studying oligomers of specific size (Fig. 4D). In addition to using different geometries, force probes may be operated in different modalities. The most common is to ramp the force up to unfold the structure. Plotting the resulting force-extension curve (FEC), a "rip" arising from an abrupt increase in the molecular extension reveals an unfolding event (Fig. 5A). The change in contour length during the rip indicates the size of the structure being unfolded, whereas the unfolding force relates to the stability of the structure, the unfolding kinetics, and the properties of the energy landscape.[102] Instead of ramping the force gradually, the force can be jumped suddenly and then kept constant with an active or passive force clamp.[103] Such force-jump measurements[104] are a more sensitive way of observing intermediate structures, but the need for a force clamp adds technical complexity. In both of these modalities, the structural transitions are out of equilibrium due to the fast changes in the force. Measurements in which the molecules are kept in equilibrium at all times are also possible, by keeping either force or probe separation constant during the measurement (Fig. 5B). This modality has been used very successfully to study structure formation,[99,101] but it is most appropriate for processes that are relatively rapid at equilibrium, to avoid impractically-long measurement times.

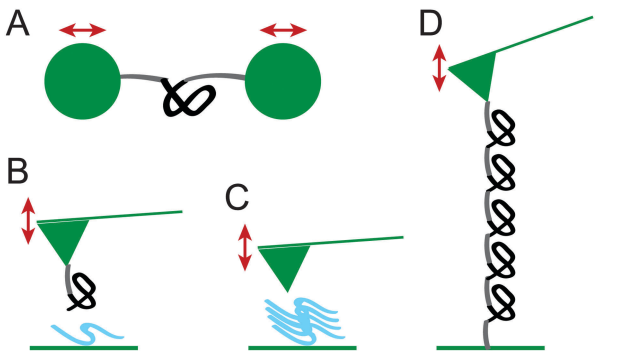

Fig. 4 Schematic representation of single-molecule force spectroscopy assays. (A) A single molecule (black) is attached to the probe (here optical tweezers) *via* handles to study monomer misfolding. (B) A monomer (black) bound to an AFM tip (green) is brought into contact with a monomer or aggregate (blue) attached to the surface to probe the interaction between them. (C) An AFM tip is used to pull on part of an aggregate (blue) stuck to a surface. (D) A tandem-repeat oligomer, consisting of multiple copies of the protein (black) connected end to end, is pulled on by a force probe (here, AFM).

The application of force to specific locations on the protein has both benefits and disadvantages. The denaturant can be targeted to a specific region of the protein, effectively selecting for particular pathways in a controllable way. Such selection allows a detailed exploration of the microscopic drivers of aggregation, but discerning the biological relevance of a given pathway can be challenging. An attractive feature of force spectroscopy is that the force-dependence of quantities such as the rates and occupancies of different states can be used to quantify the fundamental energy landscape underlying folding and aggregation, whether in terms of critical parameters such as barrier heights and locations[102] or the full profile of the landscape.[105–108] The rates can also be extrapolated to zero force for comparison to other assays, but such extrapolations must be interpreted carefully to account for effects such as changes in the nature of the barrier with force.[109] As a consequence of the one-dimensional nature of the measurement, structural rearrangements that don't change the extension of the molecule between the chosen attachment points will not be observed; "hidden" intermediates like these may, however, be revealed by changing the attachment points.[110]

The force probes themselves introduce a number of technical challenges. For example, in many cases the protein is tethered to the probe *via* the sulfhydryl group of a natural or engineered cysteine residue.[111] Such tethering may alter the aggregation behavior of the protein, either through the changes to the protein or the presence of the tether; useful controls to test for these effects include ensemble aggregation measurements and changing the molecule used as a tether. In other cases, the protein is attached to the probe by non-specific adsorption (*e.g.* to an AFM tip) or specific non-covalent interactions (*e.g.* avidin binding to a biotin label on the protein). The proximity to the surface of the probe may introduce spurious interactions between the protein and the probe that may alter the aggregation. It is thus best to use spacers to separate the protein from nearby surfaces.

The main applications of force spectroscopy in the context of aggregation have been: (i) identification and characterization of misfolded protein monomers, as precursors to aggregation; (ii) characterizing the structures that form in small oligomers and the interactions between monomers within them; and (iii) characterizing the interactions within amyloid fibrils and their structural properties. Many of these studies have focused on disease-related proteins, especially α-synuclein, aβ,

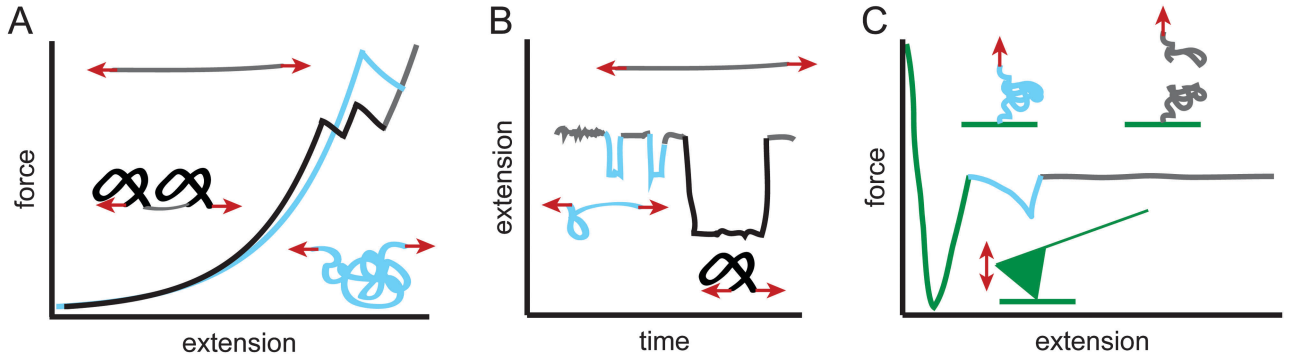

Fig. 5 Schematic results from single-molecule force measurements. (A) Force-extension curves (FECs): Rips in the traces where the extension jumps suddenly represent single unfolding events. The number and sizes of the rips can be related to native (black) or non-native (blue) conformations (gray: unfolded state). Here, the unfolding of a dimer is illustrated: the native structure unfolds in two equal steps, whereas the non-native structure unfolds in a single step. (B) Trajectory of the extension of a molecule held at constant force. Different conformations appear with different extensions and lifetimes. (C) FEC of the dissociation between two domains, as in the assays from Fig. 4B and C. An initial peak shows the interaction of tip and surface (green), a second peak reflects the stretching of the tethered molecule (blue). When the molecule attached to the tip dissociates from the aggregate, the force jumps to zero (gray).

and prion proteins. We discuss examples of each of these applications using AFM and optical tweezers.

Monomer misfolding studies

The misfolding of monomers has been measured for a variety of different proteins. AFM was used to observe the misfolding of the Na+/H+ antiporter membrane protein NhaA, immobilizing the protein in a membrane tethered to a mica surface.[112] About 15% of the refolding events led to a state displaying non-native characteristics, judged by the change in the contour length of the molecule upon unfolding. AFM has also been used to study misfolding in α-synuclein monomers sandwiched between tandem-repeat oligomers of I27.[113,114] Three types of features that did not correspond to I27 unfolding were observed in the FECs: unfolding events at high force (~200 pN), assigned tentatively to a β-like conformation; events at lower forces (~60 pN), indicating mechanically weaker interactions; and unfolding records with no resolvable transition, assigned to a random-coil state. Interestingly, the "β-like" conformation was more prevalent under aggregation-prone conditions—such as low pH, high ionic strength, and presence of disease-associated mutations.

Recently, high-resolution optical tweezers have been applied to identify and characterize misfolded states in protein monomers using both force-ramp (Fig. 5A) and equilibrium (Fig. 5B) measurements. Measurements of calmodulin, which consists of two domains connected by a flexible linker, found no evidence for misfolding within the isolated domains, but identified two rare misfolded structures driven by inter-domain interactions.[115] These states were distinguished by having different force-dependent kinetics and/or lengths, and were further characterized by using deletion mutants to determine which parts of the protein were misfolded. Studies of the coiled-coil proteins pIL and pER found that staggered pairing of the helices produced multiple misfolded structures.[116] Hidden Markov modeling of the data suggested up to three misfolded states, populated up to 2% of the time under tension. Folding of the prion protein PrP has also been studied with optical tweezers, which is especially interesting because PrP can misfold into an infectious agent.[117] Although no intermediates were found on the native folding pathway, multiple pathways leading from the unfolded state to three different misfolded states were observed. The misfolded states were very short-lived compared to the native state and hence much less stable; some were occupied as little as 0.04% of the time. The misfolding lifetimes were increased in a mutant with enhanced aggregation propensity. An independent kinetic analysis using signal-pair correlation analysis confirmed that the misfolded states were indeed not on the pathway to the native structure.[118]

These studies show that force spectroscopy can be a powerful and very sensitive probe of monomer misfolding. As with other single-molecule approaches, using isolated molecule allows the folding to be observed under conditions where the protein would otherwise aggregate rapidly, providing a more complete exploration of the properties of the monomeric protein that may trigger aggregation. However, these studies also highlight some of the technical factors that may affect interpretation. For example, the attachment of handles may constrain the structures that can be formed, as discussed above. Moreover, if additional molecules are present, such as mechanically-stable "reference" proteins or DNA handles, one must check that they do not interact with the protein of interest leading to structural artifacts (in addition to potential interactions with nearby surfaces).

Studying the interactions driving dimerization

In addition to studying non-native structures formed by monomeric proteins, force spectroscopy has been used to study the interactions between monomers leading to dimers, as a likely first step in aggregation. To do this, monomers were attached separately to a force probe as well as to a functionalized surface (Fig. 4B). The molecules on the surface and probe were then brought into physical contact to form a dimer before being pulled apart (Fig. 5C). The Lyubchenko group used this

approach to study the interactions between α-synuclein molecules by measuring FECs with AFM. They observed an increase in force with extension followed by a rupture event as the monomers were pulled apart,[119–122] with the rupture force distribution varying with pH[121] and the presence of polyamines[122] or metal ions.[123] The contour length of the dimer was estimated by fitting the FECs to a polymer model and used to suggest structural models of the dimer. The same approach was applied to aβ[119,124] and a peptide from the yeast prion protein Sup35.[125] The unfolding kinetics for the intermolecular interactions were extracted from the average rupture force at various pulling rates.[126] In all cases, the dimer lifetimes increased with decreasing pH or increasing ionic strength, indicating stronger interactions under those conditions.

The ability to isolate dimers as minimal aggregates for studying intermolecular interactions is a key advantage of this assay. One challenge is that weak interactions are difficult to resolve, both due to the likely presence of non-specific interactions between the protein and the surface or tip, and the fact that AFM is not well-suited to measure small forces. Characterizing the structures formed by the dimers in such assays is also challenging, because the structure in the dimer may not completely unfold before the two monomers dissociate.

Studies of non-native oligomerization in tandem proteins

Instead of bringing two molecules into contact by physical manipulation with the force probe, intermolecular interactions can be probed by linking monomers together to form tandem-repeat oligomers (Fig. 4D). Such an approach provides several advantages. First, oligomers larger than dimers may be studied. More importantly, it makes it easier to characterize the structures that are formed within an oligomeric aggregate, since one can ensure that the constituent monomers are unfolded completely in each measurement and thereby determine the full contour length change upon unfolding. Different proteins may also be included in the chain, to probe co-aggregation.

When studying the native folding of a tandem-repeat oligomer of I27 with AFM, Oberhauser *et al.* found that a small fraction (~2%) of the FECs displayed about twice the expected contour length, which was interpreted in terms of the formation of a non-native dimer.[127] Dougan *et al.* later observed similar misfolded states in the same construct,[128] though again only occasionally, in the presence of 2,2,2-trifluoroethanol, a compound that enhanced misfolding and aggregation of I27 domains in bulk studies. This misfolded dimer might be the same as that recently studied by single-molecule FRET.[93] In a similar vein, interactions between the domains in polyproteins (tandem constructs containing different proteins linked together) have also been measured with AFM. Randles *et al.* observed misfolding of the R16 and R17 domains of spectrin,[129] whereas Kaiser *et al.* probed the misfolding of titin I27 upon interaction with the motor domain from myosin.[130] AFM experiments on tandem repeats have also been used to probe the role of interactions such as disulfide bonds, observing the formation of non-native oligomeric structures as a result of disulfide bond formation between adjacent domains of human cardiac titin I27.[131]

Tandem-repeats have been used to study oligomerization in optical tweezers experiments as well. Bechtluft *et al.* observed the aggregation of maltose binding protein (MBP) and the effect of the chaperone SecB.[132] In the absence of the chaperone, a tandem tetramer of MBP was often found to form an aggregated structure with a higher unfolding force than native MBP. The aggregate was prevented by SecB binding. Recently, Yu *et al* observed non-native structures formed by dimers and trimers of PrP, finding multiple intermediates in the unfolding of these structures in contrast to two-state unfolding for native PrP.[62]

Such measurements of non-native structures in tandem-repeat oligomers provide a revealing view into the mechanisms of structure formation during the early steps of aggregation, including a direct comparison between the probability of forming non-native *vs.* native structures. In contrast to other methods for studying oligomers, here the size of the oligomer is controlled by the design of the protein constructs being measured. This allows the behavior of oligomers of certain sizes to be characterized in isolation, thereby enabling a reductionist approach to the complex phenomenon of aggregation. The cost of this control, however, is that the tethering of the proteins (both to the force probe and to the other proteins within an oligomer) imposes geometrical constraints on the structures that may form, potentially changing the behavior. Additional experiments are thus needed to elucidate the differences in behavior induced by the geometrical constraints. For example, the ability of tandem oligomers to replicate the properties of aggregates formed by the unlinked protein can be ascertained (as done with tandem dimers of the SH3 domain discussed above, which readily formed fibrils[133]), or the toxicity of tandem oligomers can be tested in the case of disease-related aggregation (as done with tandem dimers of PrP[134]). The constraints imposed by the linkers can also be explored by mapping the effects of changing the linking topology as well as the position, length, and composition of the linkers.

Studies of amyloid fibrils

Whereas the behavior of monomers and oligomers is important for understanding the early stages of aggregation, amyloid fibrils are interesting since they often represent its end-point. Amyloids are typically very stable, however, which makes it challenging to probe the interactions between and within the molecules forming the fibril. Force spectroscopy provides a unique means to do so, because sufficiently high forces can be applied to break even the strongest bonds. Studies of the mechanical properties of single fibrils (especially using AFM) have been reviewed elsewhere recently.[135] Here, we concentrate on measurements of the interactions within the fibril using both AFM and optical tweezers.

In AFM force spectroscopy, the fibrils are typically attached to a surface, and the AFM tip is used to pull the fibril apart by grabbing onto part of the fibril *via* either specific or non-specific attachments (Fig. 4C). Dong *et al.* pulled on fibrils

made of glucagon,[136] finding that they ruptured at around 200 pN. However, the use of non-specific attachments produced a diverse population of FECs, complicating the interpretation. By engineering a cysteine residue into human PrP, Ganchev *et al.* formed a specific attachment to a gold-coated tip. Pulling monomers out from PrP fibrils, they found that the behavior was similar to that for shearing β-structured proteins, suggesting that the core of the PrP had changed from helical in the monomer to β-sheet in the fibril.[137] Similar measurements of fibrils formed from aβ revealed that they could withstand much less force, with the unfolding force depending on the peptide fragment used to make the fibril: aβ(1–40) unfolded around 30 pN, whereas aβ(1–42) unfolded around 20 pN.[138,139] More interestingly, in aβ fibrils the subunits were unfolded and refolded in rapid equilibrium, generating a reproducible plateau in FECs at different forces; this rapid equilibrium might play some role in aggregate assembly.

Dong *et al.* characterized the intermolecular interactions in fibrils made of Sup35 using optical tweezers at high force.[140] Here, a variant of the assay in Fig. 4B was used: a monomer tethered to a bead was incorporated *via* self-assembly into a fibril, which was in turn immobilized on a microscope cover-glass. Surprisingly, the interactions between the monomers comprising the fibril were found to be stronger than the interactions within the individual folded monomers. The regions involved in the key interactions were mapped by making fibrils from mutants. Subsequent work showed that fibrils from two different prion strains had different mechanical characteristics such as stiffness and persistence length.[141]

These experiments show that force spectroscopy can give insight into the interactions that make fibrils so stable and the structural properties of the monomers within the amyloid. Another strength of such assays, given the potential applications of amyloids as biomaterials,[142] is the ability to characterize the mechanical properties of the fibrils. However, it can be challenging to discern the implications of measurements like these for the fibril structure. As with the dimer dissociation assays, monomers pulled out of a fibril may not unfold completely before dissociating. Moreover, the unfolding of multiple segments of the fibril at once may lead to very broad distributions of unfolding lengths, complicating the interpretation. Additional experiments such as mutational analysis or changes to the attachment point locations may help address these issues.

Nanopore analysis

Another single-molecule technique that has recently been applied to study protein aggregation is nanopore analysis. Here, nanopores are introduced into a lipid membrane[143] (typically using a pore-forming protein such as α-hemolysin) or a solid-state membrane (typically using silicon nanofabrication).[144] A voltage clamp applied across the membrane drives an ionic current through the nanopore; as protein molecules associate with the pore or translocate through it, the current level is reduced.[144] Since different structures can modulate the current in different ways, information can be gained about the conformational distribution in the sample.

α-Hemolysin pores were used to probe the conformational variability of aβ, α-synuclein, and human and bovine PrP.[143,145,146] Changes in the ion current were related to changes in the conformations resulting from disease-related mutations or the binding of small molecules. Owing to the small size of the pores (~1.5 nm diameter), however, these studies were restricted to monomers and small oligomers. Yusko *et al.* developed larger synthetic nanopores capable of characterizing oligomers and even fibrils formed by aβ.[147] A lipid-bilayer coating reduced clogging of the pores due to non-specific interactions and also allowed the pore diameter to be fine-tuned.[148] Different current levels and blockage times were interpreted as translocation events corresponding to spherical oligomers, cylindrical protofibrils, or fibrils. Interestingly, pores formed by α-synuclein oligomers themselves could be analyzed with a similar approach:[149] adding oligomeric α-synuclein into lipid bilayers resulted in quantized changes in the conductance, consistent with pore formation.

Nanopore assays have the advantage that the protein does not need to be labeled. Oligomers of a given size can in principle be selected by tuning the pore size, a feature which will be aided by advances in artificial pores (such as those made lithographically or with DNA origami[150]). A principal challenge, in addition to the possibility of interactions with the pore and nearby surface, is that it can be difficult to relate blockade currents to structures, especially when the possible structures are themselves unknown.

Summary

Single-molecule techniques have been successfully applied to investigate a variety of questions about protein misfolding and aggregation in different systems. A broad overview of the assays described here and their suitability for addressing specific questions is shown in Table 1. In general, misfolding of protein monomers is best probed with force-based techniques and FRET, since these methods can identify low fractions of misfolded conformations in the presence of other conformations. Optical tweezers and FRET, especially, can provide detailed information about the structural, thermodynamic, and kinetic features of these misfolded states. Oligomerization in the early stages of aggregation can be investigated with all methods. In force-based assays using tandem constructs, oligomers of defined size can be unfolded and refolded repeatedly for their characterization. In the fluorescence-based assays, oligomerization is typically observed in a kinetic measurement. Here, FCS and burst-size-based assays can reveal size distributions as a function of time, whereas FRET can give more detailed information about inter- or intra-molecular distances and other structural features. The same information can in principle be gained from FRET experiments with larger aggregates as well. Force spectroscopy is particular suited to characterizing the strong interactions within amyloid fibrils. Single-molecule assays can thus be applied to all stages of protein misfolding

Table 1 Overview of different single-molecule assays. Complete details are in the main text

Technique	Single-molecule assay	Process studied	Typical protein attachment	Information available
Fluorescence	FCS	Oligomerization	Fluorescent dye	Diffusion time, species abundance,...
	Dual-probe intensity	Oligomerization	Two dyes	Oligomer size distribution, formation kinetics,...
	FRET	Misfolding, oligomerization, aggregation	Donor–acceptor dye pair	Molecular distances, chain dynamics,...
Force	Monomer misfolding	Misfolding	AFM tip and surface, bead and surface, or two beads	Molecular distances, energies, barrier heights, rates,...
	Tandem oligomer, dimer	Misfolding, oligomerization		
	Amyloid fiber	Aggregation	Surface	
Other	Nanopore analysis	Misfolding, oligomerization	None	Formation kinetics

and aggregation, revealing detailed information about the underlying processes.

Next to the specific capabilities of the assays, the degree to which the molecule of interest must be modified for the measurements is another important characteristic. Examples include the attachment of dyes in the fluorescence-based assays, the attachment of other molecules as ''handles'' in force-based assays, and surface immobilization in some force- and fluorescence-based assays. An inevitable control in all these experiments is to check whether these modifications affect the process being investigated.

Outlook

Despite the advantages offered by single-molecule techniques, their application to study protein misfolding and aggregation is still in its infancy. This is partly due to the high technical demands of these methods, both in terms of the often complex instrumentation as well as the biochemical modifications of the proteins required for most of the assays. In addition, the data analysis methods needed are typically sophisticated, reflecting the complexity of the underlying behavior. Technical advances resulting in the development of more standardized instrumentation, assay design, and data analysis will be particularly helpful for widening the adoption of these methods. Continued technical improvements will also likely lead to increased resolution and sensitivity, allowing new and more detailed information to be extracted. Another avenue to enhance the impact of single-molecule studies is by coupling them with computational simulations:[151] the molecular-scale detail in the experimental results may provide very useful constraints for simulating a complex problem, similar to recent work using FRET measurements to constrain simulations of intrinsically-disordered α-synuclein.[152] In addition, the application of single-molecule techniques has been concentrated on cases where aggregation is an undesirable outcome as in disease, although the methods are equally suitable to native aggregation and might shed new lights on possible differences. A key challenge going forward is relating the unique information provided by single-molecule experiments to the picture provided by ensemble assays, and in particular connecting the structural and dynamic features observed in single molecules and oligomers *in vitro* to the overall outcomes of aggregation *in vivo*.

Acknowledgements

This work was supported by Canadian Institutes of Health Research (CIHR) grant reference number NHG 91374, the *nanoWorks* program of Alberta Innovates, and the National Institute for Nanotechnology. A.H. acknowledges fellowship support from CIHR and Alberta Innovates Health Solutions.

Notes and references

1 C. M. Dobson, *Semin. Cell Dev. Biol.*, 2004, **15**, 3–16.
2 R. Jaenicke, *Philos. Trans. R. Soc. London, Ser. B*, 1995, **348**, 97–105.
3 E. Monsellier and F. Chiti, *EMBO Rep.*, 2007, **8**, 737–742.
4 B. Hardesty, T. Tsalkova and G. Kramer, *Curr. Opin. Struct. Biol.*, 1999, **9**, 111–114.
5 F. U. Hartl, A. Bracher and M. Hayer-Hartl, *Nature*, 2011, **475**, 324–332.
6 N. F. S. Bence, *Science*, 2001, **292**, 1552.
7 J. Tyedmers, A. Mogk and B. Bukau, *Nat. Rev. Mol. Cell Biol.*, 2010, **11**, 777–788.
8 R. Rudolph and H. Lilie, *FASEB J.*, 1996, **10**, 49–56.
9 S. Frokjaer and D. E. Otzen, *Nat. Rev. Drug Discovery*, 2005, **4**, 298–306.
10 W. Wang, *Int. J. Pharm.*, 2005, **289**, 1–30.
11 G. B. Bolli, R. D. Di Marchi, G. D. Park, S. Pramming and V. A. Koivisto, *Diabetologia*, 1999, **42**, 1151–1167.
12 M. Ramirez-Alvarado, J. W. Kelly and C. M. Dobson, *Protein Misfolding Diseases: Current and Emerging Principles and Therapies*, John Wiley & Sons, 2010.
13 R. Nelson, M. R. Sawaya, M. Balbirnie, A. Madsen, C. Riekel, R. Grothe and D. Eisenberg, *Nature*, 2005, **435**, 773–778.
14 F. Chiti and C. M. Dobson, *Annu. Rev. Biochem.*, 2006, **75**, 333–366.
15 B. Caughey and P. T. Lansbury, *Annu. Rev. Neurosci.*, 2003, **26**, 267–298.
16 C. G. Glabe, *J. Biol. Chem.*, 2008, **283**, 29639–29643.

17 J. Bieschke, M. Herbst, T. Wiglenda, R. P. Friedrich, A. Boeddrich, F. Schiele, D. Kleckers, J. M. L. del Amo, B. A. Grüning, Q. Wang, M. R. Schmidt, R. Lurz, R. Anwyl, S. Schnoegl, M. Fändrich, R. F. Frank, B. Reif, S. Günther, D. M. Walsh and E. E. Wanker, *Nat. Chem. Biol.*, 2012, **8**, 93–101.
18 D. M. Fowler, A. V. Koulov, W. E. Balch and J. W. Kelly, *Trends Biochem. Sci.*, 2007, **32**, 217–224.
19 T. Eichner and S. E. Radford, *Mol. Cell*, 2011, **43**, 8–18.
20 B. L. Kagan, *in Molecular Biology of Neurodegenerative Diseases*, Academic Press, 2012, vol. 107, pp. 295–325.
21 H. Olzscha, S. M. Schermann, A. C. Woerner, S. Pinkert, M. H. Hecht, G. G. Tartaglia, M. Vendruscolo, M. Hayer-Hartl, F. U. Hartl and R. M. Vabulas, *Cell*, 2011, **144**, 67–78.
22 J. Winkler, A. Seybert, L. König, S. Pruggnaller, U. Haselmann, V. Sourjik, M. Weiss, A. S. Frangakis, A. Mogk and B. Bukau, *EMBO J.*, 2010, **29**, 910–923.
23 M. Goedert, F. Clavaguera and M. Tolnay, *Trends Neurosci.*, 2010, **33**, 317–325.
24 G. Natale, M. Ferrucci, G. Lazzeri, A. Paparelli and F. Fornai, *Prion*, 2011, **5**, 142–149.
25 M. W. Miller and E. S. Williams, *Nature*, 2003, **425**, 35–36.
26 A. Aguzzi and L. Rajendran, *Neuron*, 2009, **64**, 783–790.
27 L. I. Grad, W. C. Guest, A. Yanai, E. Pokrishevsky, M. A. O'Neill, E. Gibbs, V. Semenchenko, M. Yousefi, D. S. Wishart, S. S. Plotkin and N. R. Cashman, *Proc. Natl. Acad. Sci. U. S. A.*, 2011, **108**, 16398–16403.
28 J. Stöhr, J. C. Watts, Z. L. Mensinger, A. Oehler, S. K. Grillo, S. J. DeArmond, S. B. Prusiner and K. Giles, *Proc. Natl. Acad. Sci. U. S. A.*, 2012, **109**, 11025–11030.
29 C. J. Roberts, *Biotechnol. Bioeng.*, 2007, **98**, 927–938.
30 A. M. Morris, M. A. Watzky and R. G. Finke, *Biochim. Biophys. Acta, Proteins Proteomics*, 2009, **1794**, 375–397.
31 R. Kodali and R. Wetzel, *Curr. Opin. Struct. Biol.*, 2007, **17**, 48–57.
32 R. Wetzel, *Cell*, 1996, **86**, 699–702.
33 L. Narhi, S. J. Wood, S. Steavenson, Y. Jiang, G. M. Wu, D. Anafi, S. A. Kaufman, F. Martin, K. Sitney, P. Denis, J. C. Louis, J. Wypych, A. L. Biere and M. Citron, *J. Biol. Chem.*, 1999, **274**, 9843–9846.
34 I. Baskakov, P. Disterer, L. Breydo, M. Shaw, A. Gill, W. James and A. Tahiri-Alaoui, *FEBS Lett.*, 2005, **579**, 2589–2596.
35 C. R. Ellis, B. Maiti and W. G. Noid, *J. Am. Chem. Soc.*, 2012, **134**, 8184–8193.
36 N. M. Valette, S. E. Radford, S. A. Harris and S. L. Warriner, *Chembiochem*, 2012, **13**, 271–281.
37 D. W. Bolen and I. V. Baskakov, *J. Mol. Biol.*, 2001, **310**, 955–963.
38 H.-X. Zhou, G. Rivas and A. P. Minton, *Annu. Rev. Biophys.*, 2008, **37**, 375–397.
39 D. Shukla, C. P. Schneider and B. L. Trout, *Adv. Drug Delivery Rev.*, 2011, **63**, 1074–1085.
40 C. M. Dobson, *Methods*, 2004, **34**, 4–14.
41 M. Nilsson, *Methods*, 2004, **34**, 151–160.
42 L. Giehm, N. Lorenzen and D. E. Otzen, *Methods*, 2011, **53**, 295–305.
43 S. Gregoire, J. Irwin and I. Kwon, *Korean. J. Chem. Eng.*, 2012, **29**, 693–702.
44 A. Borgia, P. M. Williams and J. Clarke, *Annu. Rev. Biochem.*, 2008, **77**, 101–125.
45 A. C. M. Ferreon and A. A. Deniz, *Biochim. Biophys. Acta, Proteins Proteomics*, 2011, **1814**, 1021–1029.
46 W. E. Moerner and M. Orrit, *Science*, 1999, **283**, 1670–1676.
47 M. Böhmer and J. Enderlein, *ChemPhysChem*, 2003, **4**, 792–808.
48 R. Roy, S. Hohng and T. Ha, *Nat. Methods*, 2008, **5**, 507–516.
49 D. Duzdevich and E. C. Greene, *Philos. Trans. R. Soc. London, Ser. B*, 2013, **368**, DOI: 10.1098/rstb.2012.0248.
50 I. Rasnik, S. A. McKinney and T. Ha, *Acc. Chem. Res.*, 2005, **38**, 542–548.
51 H. S. Chung, J. M. Louis and W. A. Eaton, *Proc. Natl. Acad. Sci. U. S. A.*, 2009, **106**, 11837–11844.
52 A. E. Cohen and W. E. Moerner, *Proc. Natl. Acad. Sci. U. S. A.*, 2006, **103**, 4362–4365.
53 M. Kinoshita, K. Kamagata, A. Maeda, Y. Goto, T. Komatsuzaki and S. Takahashi, *Proc. Natl. Acad. Sci. U. S. A.*, 2007, **104**, 10453–10458.
54 A. Hoffmann, D. Nettels, J. Clark, A. Borgia, S. E. Radford, J. Clarke and B. Schuler, *Phys. Chem. Chem. Phys.*, 2011, **13**, 1857–1871.
55 C. Liu, Y. Qu, Y. Luo and N. Fang, *Electrophoresis*, 2011, **32**, 3308–3318.
56 Y. Gambin, V. VanDelinder, A. C. M. Ferreon, E. A. Lemke, A. Groisman and A. A. Deniz, *Nat. Methods*, 2011, **8**, 239–241.
57 D. Nettels, A. Hoffmann and B. Schuler, *J. Phys. Chem. B*, 2008, **112**, 6137–6146.
58 T. Ha, T. A. Laurence, D. S. Chemla and S. Weiss, *J. Phys. Chem. B*, 1999, **103**, 6839–6850.
59 B. Schuler and W. A. Eaton, *Curr. Opin. Struct. Biol.*, 2008, **18**, 16–26.
60 E. Sisamakis, A. Valeri, S. Kalinin, P. J. Rothwell and C. A. M. Seidel, in *Single Molecule Tools, Part B: Super-Resolution, Particle Tracking*, Multiparameter and Force Based Methods, Academic Press, 2010, vol. 475, pp. 455–514.
61 A. J. Trexler and E. Rhoades, *Mol. Neurobiol.*, 2013, **47**, 622–631.
62 H. Yu, D. R. Dee and M. T. Woodside, *Prion*, 2013, **7**, 140–146.
63 O. Krichevsky and G. Bonnet, *Rep. Prog. Phys.*, 2002, **65**, 251–297.
64 E. Haustein and P. Schwille, *Annu. Rev. Biophys. Biomol. Struct.*, 2007, **36**, 151–169.
65 K. Post, M. Pitschke, O. Schäfer, H. Wille, T. R. Appel, D. Kirsch, I. Mehlhorn, H. Serban, S. B. Prusiner and D. Riesner, *Biol. Chem.*, 1998, **379**, 1307–1317.
66 L. O. Tjernberg, A. Pramanik, S. Björling, P. Thyberg, J. Thyberg, C. Nordstedt, K. D. Berndt, L. Terenius and R. Rigler, *Chem. Biol.*, 1999, **6**, 53–62.

67 P. Sengupta, K. Garai, B. Sahoo, Y. Shi, D. J. E. Callaway and S. Maiti, *Biochemistry*, 2003, **42**, 10506–10513.
68 P. Sengupta, K. Garai, J. Balaji, N. Periasamy and S. Maiti, *Biophys. J.*, 2003, **84**, 1977–1984.
69 S. Nag, J. Chen, J. Irudayaraj and S. Maiti, *Biophys. J.*, 2010, **99**, 1969–1975.
70 M. Gerard, Z. Debyser, L. Desender, P. J. Kahle, J. Baert, V. Baekelandt and Y. Engelborghs, *FASEB J.*, 2006, **20**, 524–526.
71 S. Nath, J. Meuvis, J. Hendrix, S. A. Carl and Y. Engelborghs, *Biophys. J.*, 2010, **98**, 1302–1311.
72 J. Enderlein, I. Gregor, D. Patra and J. Fitter, *Curr. Pharm. Biotechnol.*, 2004, **5**, 155–161.
73 E. P. Petrov and P. Schwille, in *Standardization and Quality Assurance in Fluorescence Measurements II*, ed. U. Resch-Genger, Springer Berlin Heidelberg, 2008, vol. 6, pp. 145–197.
74 J. D. Lam, M. J. Culbertson, N. P. Skinner, Z. J. Barton and D. L. Burden, *Anal. Chem.*, 2011, **83**, 5268–5274.
75 U. Meseth, T. Wohland, R. Rigler and H. Vogel, *Biophys. J.*, 1999, **76**, 1619–1631.
76 T. Dertinger, V. Pacheco, I. von der Hocht, R. Hartmann, I. Gregor and J. Enderlein, *Chemphyschem*, 2007, **8**, 433–443.
77 I. Gregor and J. Enderlein, *Photochem. Photobiol. Sci.*, 2007, **6**, 13–18.
78 M. Pitschke, R. Prior, M. Haupt and D. Riesner, *Nat. Med.*, 1998, **4**, 832–834.
79 J. Bieschke, A. Giese, W. Schulz-Schaeffer, I. Zerr, S. Poser, M. Eigen and H. Kretzschmar, *Proc. Natl. Acad. Sci. U. S. A.*, 2000, **97**, 5468–5473.
80 E. Birkmann, O. Schäfer, N. Weinmann, C. Dumpitak, M. Beekes, R. Jackman, L. Thorne and D. Riesner, *Biol. Chem.*, 2006, **387**, 95–102.
81 S. A. Funke, E. Birkmann, F. Henke, P. Görtz, C. Lange-Asschenfeldt, D. Riesner and D. Willbold, *Biochem. Biophys. Res. Commun.*, 2007, **364**, 902–907.
82 A. Giese, B. Bader, J. Bieschke, G. Schaffar, S. Odoy, P. J. Kahle, C. Haass and H. Kretzschmar, *Biochem. Biophys. Res. Commun.*, 2005, **333**, 1202–1210.
83 J. Levin, U. Bertsch, H. Kretzschmar and A. Giese, *Biochem. Biophys. Res. Commun.*, 2005, **329**, 1200–1207.
84 M. Kostka, T. Högen, K. M. Danzer, J. Levin, M. Habeck, A. Wirth, R. Wagner, C. G. Glabe, S. Finger, U. Heinzelmann, P. Garidel, W. Duan, C. A. Ross, H. Kretzschmar and A. Giese, *J. Biol. Chem.*, 2008, **283**, 10992–11003.
85 A. S. Hillmer, P. Putcha, J. Levin, T. Högen, B. T. Hyman, H. Kretzschmar, P. J. McLean and A. Giese, *Biochem. Biophys. Res. Commun.*, 2010, **391**, 461–466.
86 T. Högen, J. Levin, F. Schmidt, M. Caruana, N. Vassallo, H. Kretzschmar, K. Bötzel, F. Kamp and A. Giese, *Biophys. J.*, 2012, **102**, 1646–1655.
87 B. Bader, G. Nübling, A. Mehle, S. Nobile, H. Kretzschmar and A. Giese, *Biochem. Biophys. Res. Commun.*, 2011, **411**, 190–196.
88 M. Duering, A. Karpinska, S. Rosner, F. Hopfner, M. Zechmeister, N. Peters, E. Kremmer, C. Haffner, A. Giese, M. Dichgans and C. Opherk, *Hum. Mol. Genet.*, 2011, **20**, 3256–3265.
89 A. Orte, N. R. Birkett, R. W. Clarke, G. L. Devlin, C. M. Dobson and D. Klenerman, *Proc. Natl. Acad. Sci. U. S. A.*, 2008, **105**, 14424–14429.
90 P. Narayan, A. Orte, R. W. Clarke, B. Bolognesi, S. Hook, K. A. Ganzinger, S. Meehan, M. R. Wilson, C. M. Dobson and D. Klenerman, *Nat. Struct. Mol. Biol.*, 2012, **19**, 79–83.
91 A. J. Trexler and E. Rhoades, *Biophys. J.*, 2010, **99**, 3048–3055.
92 A. C. M. Ferreon, C. R. Moran, J. C. Ferreon and A. A. Deniz, *Angew. Chem., Int. Ed.*, 2010, **49**, 3469–3472.
93 M. B. Borgia, A. Borgia, R. B. Best, A. Steward, D. Nettels, B. Wunderlich, B. Schuler and J. Clarke, *Nature*, 2011, **474**, 662–665.
94 F. Hillger, D. Nettels, S. Dorsch and B. Schuler, *J. Fluoresc.*, 2007, **17**, 759–765.
95 N. Cremades, S. I. A. Cohen, E. Deas, A. Y. Abramov, A. Y. Chen, A. Orte, M. Sandal, R. W. Clarke, P. Dunne, F. A. Aprile, C. W. Bertoncini, N. W. Wood, T. P. J. Knowles, C. M. Dobson and D. Klenerman, *Cell*, 2012, **149**, 1048–1059.
96 K. D. Dukes, C. F. Rodenberg and R. K. Lammi, *Anal. Biochem.*, 2008, **382**, 29–34.
97 H. Ding, P. T. Wong, E. L. Lee, A. Gafni and D. G. Steel, *Biophys. J.*, 2009, **97**, 912–921.
98 B. Samorì, G. Zuccheri and P. Baschieri, *Chemphyschem*, 2005, **6**, 29–34.
99 K. C. Neuman and A. Nagy, *Nat. Methods*, 2008, **5**, 491–505.
100 M. Rief, M. Gautel, F. Oesterhelt, J. M. Fernandez and H. E. Gaub, *Science*, 1997, **276**, 1109–1112.
101 W. J. Greenleaf, M. T. Woodside and S. M. Block, *Annu. Rev. Biophys. Biomol. Struct.*, 2007, **36**, 171–190.
102 O. K. Dudko, G. Hummer and A. Szabo, *Proc. Natl. Acad. Sci. U. S. A.*, 2008, **105**, 15755–15760.
103 W. J. Greenleaf, M. T. Woodside, E. A. Abbondanzieri and S. M. Block, *Phys. Rev. Lett.*, 2005, **95**, 208102.
104 J. M. Fernandez and H. Li, *Science*, 2004, **303**, 1674–1678.
105 M. T. Woodside, P. C. Anthony, W. M. Behnke-Parks, K. Larizadeh, D. Herschlag and S. M. Block, *Science*, 2006, **314**, 1001–1004.
106 J. C. M. Gebhardt, T. Bornschlögl and M. Rief, *Proc. Natl. Acad. Sci. U. S. A.*, 2010, **107**, 2013–2018.
107 A. N. Gupta, A. Vincent, K. Neupane, H. Yu, F. Wang and M. T. Woodside, *Nat. Phys.*, 2011, **7**, 631–634.
108 H. Yu, A. N. Gupta, X. Liu, K. Neupane, A. M. Brigley, I. Sosova and M. T. Woodside, *Proc. Natl. Acad. Sci. U. S. A.*, 2012, **109**, 14452–14457.
109 O. K. Dudko, T. G. W. Graham and R. B. Best, *Phys. Rev. Lett.*, 2011, **107**, 208301.
110 E. A. Shank, C. Cecconi, J. W. Dill, S. Marqusee and C. Bustamante, *Nature*, 2010, **465**, 637–640.
111 C. Cecconi, E. Shank, F. Dahlquist, S. Marqusee and C. Bustamante, *Eur. Biophys. J.*, 2008, **37**, 729–738.
112 A. Kedrov, H. Janovjak, C. Ziegler, W. Kuhlbrandt and D. J. Muller, *J. Mol. Biol.*, 2006, **355**, 2–8.

113 M. Sandal, F. Valle, I. Tessari, S. Mammi, E. Bergantino, F. Musiani, M. Brucale, L. Bubacco and B. Samorì, *PLoS Biol.*, 2008, **6**, e6.
114 M. Brucale, M. Sandal, S. Di Maio, A. Rampioni, I. Tessari, L. Tosatto, M. Bisaglia, L. Bubacco and B. Samorì, *Chembiochem*, 2009, **10**, 176–183.
115 J. Stigler, F. Ziegler, A. Gieseke, J. C. M. Gebhardt and M. Rief, *Science*, 2011, **334**, 512–516.
116 Z. Xi, Y. Gao, G. Sirinakis, H. Guo and Y. Zhang, *Proc. Natl. Acad. Sci. U. S. A.*, 2012, **109**, 5711–5716.
117 H. Yu, X. Liu, K. Neupane, A. N. Gupta, A. M. Brigley, A. Solanki, S. Iveta and M. T. Woodside, *Proc. Natl. Acad. Sci. U. S. A.*, 2012, **109**, 5283–5288.
118 A. Hoffmann and M. T. Woodside, *Angew. Chem., Int. Ed.*, 2011, **50**, 12643–12646.
119 C. McAllister, M. Karymov, Y. Kawano, A. Lushnikov, A. Mikheikin, V. Uversky and Y. Lyubchenko, *J. Mol. Biol.*, 2005, **354**, 1028–1042.
120 J. Yu and Y. L. Lyubchenko, *J. Neuroimmune Pharmacol.*, 2008, **4**, 10–16.
121 J. Yu, S. Malkova and Y. L. Lyubchenko, *J. Mol. Biol.*, 2008, **384**, 992–1001.
122 A. V. Krasnoslobodtsev, J. Peng, J. M. Asiago, J. Hindupur, J.-C. Rochet and Y. L. Lyubchenko, *PLoS One*, 2012, **7**, e38099.
123 J. Yu, J. Warnke and Y. L. Lyubchenko, *Nanomedicine*, 2011, **7**, 146–152.
124 B.-H. Kim, N. Y. Palermo, S. Lovas, T. Zaikova, J. F. W. Keana and Y. L. Lyubchenko, *Biochemistry*, 2011, **50**, 5154–5162.
125 A. M. Portillo, A. V. Krasnoslobodtsev and Y. L. Lyubchenko, *J. Phys.: Condens. Matter*, 2012, **24**, 164205.
126 E. Evans and K. Ritchie, *Biophys. J.*, 1997, **72**, 1541–1555.
127 A. F. Oberhauser, P. E. Marszalek, M. Carrion-Vazquez and J. M. Fernandez, *Nat. Struct. Biol.*, 1999, **6**, 1025–1028.
128 L. Dougan and J. M. Fernandez, *J. Phys. Chem. A*, 2007, **111**, 12402–12408.
129 L. G. Randles, R. W. S. Rounsevell and J. Clarke, *Biophys. J.*, 2007, **92**, 571–577.
130 C. M. Kaiser, P. J. Bujalowski, L. Ma, J. Anderson, H. F. Epstein and A. F. Oberhauser, *Biophys. J.*, 2012, **102**, 2212–2219.
131 P. Kosuri, J. Alegre-Cebollada, J. Feng, A. Kaplan, A. Inglés-Prieto, C. L. Badilla, B. R. Stockwell, J. M. Sanchez-Ruiz, A. Holmgren and J. M. Fernández, *Cell*, 2012, **151**, 794–806.
132 P. Bechtluft, R. G. H. van Leeuwen, M. Tyreman, D. Tomkiewicz, N. Nouwen, H. L. Tepper, A. J. M. Driessen and S. J. Tans, *Science*, 2007, **318**, 1458–1461.
133 R. Bader, R. Bamford, J. Zurdo, B. F. Luisi and C. M. Dobson, *J. Mol. Biol.*, 2006, **356**, 189–208.
134 S. Simoneau, H. Rezaei, N. Salès, G. Kaiser-Schulz, M. Lefebvre-Roque, C. Vidal, J.-G. Fournier, J. Comte, F. Wopfner, J. Grosclaude, H. Schätzl and C. I. Lasmézas, *PLoS Pathog.*, 2007, **3**, e125.
135 K. K. M. Sweers, M. L. Bennink and V. Subramaniam, *J. Phys.: Condens. Matter*, 2012, **24**, 243101.
136 M. Dong, M. B. Hovgaard, W. Mamdouh, S. Xu, D. E. Otzen and F. Besenbacher, *Nanotechnology*, 2008, **19**, 384013.
137 D. N. Ganchev, N. J. Cobb, K. Surewicz and W. K. Surewicz, *Biophys. J.*, 2008, **95**, 2909–2915.
138 M. S. Z. Kellermayer, L. Grama, Á. Karsai, A. Nagy, A. Kahn, Z. L. Datki and B. Penke, *J. Biol. Chem.*, 2005, **280**, 8464–8470.
139 Á. Karsai, Z. Mártonfalvi, A. Nagy, L. Grama, B. Penke and M. S. Z. Kellermayer, *J. Struct. Biol.*, 2006, **155**, 316–326.
140 J. Dong, C. E. Castro, M. C. Boyce, M. J. Lang and S. Lindquist, *Nat. Struct. Mol. Biol.*, 2010, **17**, 1422–1430.
141 C. E. Castro, J. Dong, M. C. Boyce, S. Lindquist and M. J. Lang, *Biophys. J.*, 2011, **101**, 439–448.
142 S. Mankar, A. Anoop, S. Sen and S. K. Maji, *Nano Rev.*, 2011, **2**, 6032.
143 C. Madampage, O. Tavassoly, C. Christensen, M. Kumari and J. S. Lee, *Prion*, 2012, **6**, 116–123.
144 C. Dekker, *Nat. Nanotechnol.*, 2007, **2**, 209–215.
145 H.-Y. Wang, Y.-L. Ying, Y. Li, H.-B. Kraatz and Y.-T. Long, *Anal. Chem.*, 2011, **83**, 1746–1752.
146 O. Tavassoly and J. S. Lee, *FEBS Lett.*, 2012, **586**, 3222–3228.
147 E. C. Yusko, J. M. Johnson, S. Majd, P. Prangkio, R. C. Rollings, J. Li, J. Yang and M. Mayer, *Nat. Nanotechnol.*, 2011, **6**, 253–260.
148 E. C. Yusko, P. Prangkio, D. Sept, R. C. Rollings, J. Li and M. Mayer, *ACS Nano*, 2012, **6**, 5909–5919.
149 F. Schmidt, J. Levin, F. Kamp, H. Kretzschmar, A. Giese and K. Bötzel, *PLoS One*, 2012, **7**, e42545.
150 J.-P. J. Sobczak, T. G. Martin, T. Gerling and H. Dietz, *Science*, 2012, **338**, 1458–1461.
151 M. B. Prigozhin and M. Gruebele, *Phys. Chem. Chem. Phys.*, 2013, **15**, 3372–3388.
152 A. Nath, M. Sammalkorpi, D. C. DeWitt, A. J. Trexler, S. Elbaum-Garfinkle, C. S. O'Hern and E. Rhoades, *Biophys. J.*, 2012, **103**, 1940–1949.

